Heavy air pollution with the unique “non-stagnant” atmospheric boundary layer in the Yangtze River Middle Basin aggravated by regional ~~$PM_{2.5}$~~ transport of $PM_{2.5}$ over China

Chao Yu[1,2], Tianliang Zhao[1, *], Yongqing Bai[3,*], Lei Zhang[1,4], Shaofei Kong[5], Xingna Yu[1], Jinhai He[1], Chunguang Cui[3], Jie Yang[1], Yinchang You[1], Guoxu Ma[1], Ming Wu[1], Jiacheng Chang[1]

1 Collaborative Innovation Center on Forecast and Evaluation of Meteorological Disasters, Key Laboratory for Aerosol-Cloud-Precipitation of China Meteorological Administration, Nanjing University of Information Science and Technology, Nanjing 210044, China

2 Southwest Electric Power Design Institute Co., Ltd of China Power Engineering Consulting Group, Chengdu, 610021, China

3 Institute of Heavy Rain, China Meteorological Administration, Wuhan, 430205, China

4 Chengdu Academy of Environmental Sciences, Chengdu, 610031, China

5 Department of Atmospheric Sciences, School of Environmental Studies, China University of Geosciences (Wuhan), 430074, Wuhan, China

Correspondence: Tianliang Zhao (tlzhao@nuist.edu.cn); Yongqing Bai (2007byq@163.com)

Abstract: Regional transport of air pollutants controlled by both emission sources and meteorological factors results in a complex source-receptor relationship of air pollution change.

Wuhan, a metropolis~~metropolitan area~~ in the Yangtze River Middle Basin (YRMB) of central China experienced heavy air pollution characterized by excessive $PM_{2.5}$ concentrations reaching 471.1 μg m^{-3} in January 2016. In order to investigate the regional ~~$PM_{2.5}$~~ transport of $PM_{2.5}$ over China and the meteorological impact on wintertime air pollution in the YRMB area, observational meteorological and other relevant environmental data from January 2016 were analyzed. Our analysis presented the noteworthy cases of heavy $PM_{2.5}$ pollution in the YRMB area with the unique "non-stagnant" meteorological conditions of strong northerly winds, no temperature inversion and additional unstable structures in the atmospheric boundary layer. This unique set of conditions differed from the stagnant meteorological conditions characterized by near-surface weak winds, air temperature inversion, and stable structure in the boundary layer observed in heavy air pollution over most regions in China. The regional transport of $PM_{2.5}$ over central-eastern China aggravated $PM_{2.5}$ levels present in the YRMB area, thus demonstrating the source-receptor relationship between the originating air pollution regions in central-eastern China and the receiving YRMB regions. Furthermore, a backward trajectory simulation using FLEXPART-WRF to integrate the air pollutant emission inventory over China was used to explore the patterns of regional ~~$PM_{2.5}$~~ transport of $PM_{2.5}$ governed by the strong northerly winds in the cold air activity of the East Asian winter monsoon over central-eastern China, which contributes markedly to the heavy $PM_{2.5}$ pollution in the YRMB area. It was estimated that the regional ~~$PM_{2.5}$~~ transport of $PM_{2.5}$ of non-local air pollutant emissions could contribute more than 65% of the $PM_{2.5}$ concentrations to the heavy air pollution in the YRMB region during the study period, revealing the importance of the regional transport of air pollutants over central-eastern China in the formation of heavy air pollution over the YRMB region.

Key words: $PM_{2.5}$ pollution; Yangtze River Middle Basin; meteorological condition; regional transport; FLEXPART-WRF

1. Introduction

Air pollution events with excessive ambient $PM_{2.5}$ concentrations have been observed frequently in the central-eastern regions of China in recent years. These events result in serious environmental problems with adverse influence on traffic, human health, climate change and other significant aspects (Fuzzi et al., 2015; An et al., 2019; Nel, 2005). Based on the observations in China, there is a well-established association between haze pollution and high concentrations of $PM_{2.5}$ (particulate matter with an aerodynamical diameter less than 2.5 μm~~There is a well-established association in observation of China between the observation of heavy air pollution and high concentrations of PM2.5 (particulate matter with an aerodynamical diameter less than 2.5 μm~~). Air pollution levels are highly dependent on emissions of air pollutants and changes in meteorology (Tie et al., 2017; Xu et al., 2016b; An et al., 2019; Xu et al., 2016a). The accumulation~~outbreak~~, maintenance and dissipation of haze pollution events are generally determined by meteorological changes (Kan et al., 2012), among which the boundary layer structures play the most important role (Wu et al., 2017). Meteorological conditions of stagnation characterized by near-surface low winds, high humidity and stable boundary layer could govern the periodic variations of haze pollution, which present as typical wintertime air pollution in central-eastern China (Xu et al., 2016b; Zhang et al., 2014; Huang et al., 2018). Four major regions exhibiting haze pollution with high $PM_{2.5}$ concentrations and overall poor air quality are centered over North China Plain (NCP), Yangtze River Delta (YRD) in East China, Pearl River Delta (PRD) in South China and Sichuan Basin (SCB) in Southwest China (Cheng et al., 2008; Zhang et al., 2012; Deng et al., 2011; Wang et al., 2016; Tie et al., 2017; Qiao et al., 2019).

The source-receptor relationship describes the impacts of emissions from an upwind source region to pollutant concentrations or deposition at a downwind receptor location. Regional transport of source-receptor air pollutants is generally complicated by two types of factors: emission and meteorology. The emission factor includes the emission source strength, chemical transformation and production; the meteorological factor determines the transport pathway from the source to receptor regions, exchanges between boundary layer and free troposphere, the removal processes occurring over the source and receptor regions as well as along the transport pathways. Regional transport of air pollutants with the source-receptor relationship is an important issue in our understanding of changes in air quality. Driven by atmospheric circulation, the regional transport of $PM_{2.5}$ from source regions can deteriorate air quality in the downwind receptor regions, leading to the regional haze pollution observed in a large area over central-eastern China (Chang et al., 2018; Wang et al., 2014; He et al., 2017; Chen et al., 2017b; Hu et al., 2018; Jiang et al., 2015). The Yangtze River Middle Basin (YRMB) in central China is geographically surrounded by four major haze pollution regions in all directions with NCP to the north, the YRD to the east, the PRD to the south and the SCB to the west (~~see left panel of~~ Fig.1 a). Due to this specialized location of the YRMB as a regional air pollutant transport hub with subbasin topography (see ~~right panel of~~ Fig. 1b), the regional transport of air pollutants driven by the cold air activity of East Asian winter monsoonal winds in central-eastern China could develop a source-receptor relationship between major haze pollution regions (NCP, YRD, etc.) in central-eastern China and the downwind YRMB region. However, there are unresolved questions regarding the meteorological processes involved in the regional transport of air pollutants and the pattern of regional transport with contribution ~~as well as a need for an assessment of the contribution of regional transport~~ to the air quality changes observed in the YRMB.

Wuhan, a metropolis~~metropolitan area~~ located in the YRMB, has confronted the problems associated with urban air pollution, especially heavy $PM_{2.5}$ pollution events that occur in the winter (Zhong et al., 2014; Gong et al., 2015; Xu et al., 2017; Tan et al., 2015). Local emissions of air pollutants from urban transportation, industrial exhaust and bio-combustion play an important role in YRMB urban air pollution (Acciai et al., 2017; Zhang et al., 2015). Many observational and modeling studies on air pollution in this urban area have been conducted (Zheng et al., 2019; Wu et al., 2018). However, regional ~~$PM_{2.5}$~~ transport routes of $PM_{2.5}$ from central-eastern China and its contribution to air pollution over the YRMB are still poorly understood, especially in relation to heavy air pollution episodes in the YRMB area. This study ~~has~~ selected the Wuhan area as a representative area within the YRMB for investigation of the meteorological conditions of air pollution events in January 2016 and the contribution of regional ~~$PM_{2.5}$~~ transport of $PM_{2.5}$ to heavy air pollution over the YRMB region.

2. Observational analysis

2.1 Data

Wuhan, the capital of Hubei province, is located across the Yangtze River, where its surrounding water network attributed with a humid environment.~~Wuhan, the capital of Hubei province, is a metropolitan area within the YRMB located across the Yangtze River and its surrounding water~~

~~network attributed with a humid environment~~ (see ~~right panel of~~ Fig. 1b). In order to analyze the air quality change, the hourly concentrations of air pollutants including $PM_{2.5}$ in January 2016 were collected from sites over central-eastern China, including ten observational sites in Wuhan. These ten sites include nine urban sites in residential and industrial zones as well as one suburban site within the China National Air Environmental Monitoring Network. The concentrations of air pollutants were distributed spatially in less difference over the suburban and urban sites with the similar patterns and peaks of hourly changes during the heavy pollution events, demonstrating the regional heavy air pollution in a large area of the YRMB region with the contribution of regional transport from central-eastern China, while the obviously differences in air pollutant concentrations were measured with the relative high and low $PM_{2.5}$ concentrations respectively at urban sites and suburban site during the clean air period, reflecting the important influence of high air pollutant emission over urban area on local air quality. The $PM_{2.5}$ concentrations averaged over the ten observational sites were used to characterize the variations of air pollution in January 2016 over this urban area within the YRMB.

The meteorological data of surface observation and air sounding in Wuhan and other observatories in central-eastern China were obtained from the China Meteorological Data Sharing Network (http://data.cma.cn/). Meteorological data selected for this study included horizontal visibility, air temperature, relative humidity, air pressure, and wind speed and direction with temporal resolutions of 3 h for surface observation and 12 h for sounding observation in order to analyze the variations of the meteorological conditions in the atmospheric boundary layer in January 2016.

The ERA (ECMWF ReAnalysis) -Interim reanalysis data of meteorology fro~~or~~m the

ECMWF (European Centre for Medium-Range Weather Forecasts) (https://www.ecmwf.int/en/forecasts/datasets/reanalysis-datasets/) were applied to explore the cold air activity of East Asian winter monsoonal winds in January 2016 and their anomalies during heavy $PM_{2.5}$ pollution the over central-eastern China ~~the East Asian winter monsoonal winds and their anomalies over central-eastern China in January 2016~~.

2.2 Variations in $PM_{2.5}$ concentrations and meteorology in January, 2016

Based on the National Ambient Air Quality Standards of China released by the Ministry of Ecology and Environment of China in 2012 (http://www.mee.gov.cn/), light and heavy air pollution levels of $PM_{2.5}$ are categorized by ~~a~~ daily average $PM_{2.5}$ concentration exceeding 75μg ~~μg~~ m^{-3} and 150μg~~μg~~m^{-3} in ambient air, respectively. The daily variations of $PM_{2.5}$ concentrations over January 2016 in Wuhan are illustrated in ~~Figf~~Figure~~.~~ 2a. The average monthly $PM_{2.5}$ concentration reached 105.8μg ~~μg~~ m^{-3}. The national secondary standard was exceeded on 27 days with daily $PM_{2.5}$ concentrations exceeding 75μg ~~μg~~ m^{-3} during the entire month of January 2016 in Wuhan, indicating that this urban area in the YRMB was suffering under significant $PM_{2.5}$ pollution during this period. As shown in ~~Figf~~Figure~~.~~ 2a, a 21-day prolonged air pollution event resulted from high levels of daily $PM_{2.5}$ concentrations (>75μg~~μg~~ m^{-3}) over the period of January 1 to 21. During this 21-day period of air pollution, three notably heavy air pollution events occurred on January 4, 10-12 and 18 with excessive daily $PM_{2.5}$ concentrations (>150μg~~μg~~ m^{-3}); these events are marked as P1, P2 and P3 in ~~Figf~~Figure~~.~~ 2. Based on the observation in January 2016, we found ~~We observed~~ the interesting phenomenon of an apparent 7-day cycle of heavy air pollution in January 2016, reflecting an important modulation of meteorological oscillation in the East Asian winter monsoon affecting air pollution concentrations observed over the YRMB region

(Xu et al., 2016a). A period analysis on long-term observation data of air quality could provide more information on air pollution oscillations with meteorological drivers.

~~Fig~~Figure~~.~~ 2b presents the hourly changes of $PM_{2.5}$ concentrations for the three heavy air pollution events P1, P2 and P3. The heavy pollution event P1 on January 4 started at 11:00 a~~.~~m ~~.~~(local time is used for all events) and ended at 11:00 ~~p.m~~p~~.~~m~~.~~ at same day. with an observed $PM_{2.5}$ concentration peak of 471.1~~-~~μg m^{-3}. The event P2 occurred from 10:00 p~~.~~m~~.~~ on January 10 to 00:00 a.m. on January 12 with a duration of 26 h and two peaks in $PM_{2.5}$ concentrations of 231.4~~-~~μg m^{-3} and 210.6~~-~~μg m^{-3}. The event P3 was observed between 7:00 p.m. on January 17 and 2:00 p~~.~~m~~.~~ on January 18 with an explosive growth rate of 42.9~~-~~μg m^{-3} h^{-1} in $PM_{2.5}$ concentrations. Those three heavy $PM_{2.5}$ pollution episodes over the YRMB region were characterized by short durations of less than 26 h from rapid accumulation~~outbreak~~ to fast dissipation.

Using the environmental and meteorological data observed in Wuhan in January 2016, the effects of the meteorological conditions on $PM_{2.5}$ concentrations in the YRMB region were statistically analyzed in regards to hourly variations of surface $PM_{2.5}$ concentrations, near-surface wind speed (WS) and direction (WD), as well as surface air temperature (T), air pressure (P) and relative humidity (RH) (Fig. 3). Among the observed hourly changes in $PM_{2.5}$ concentrations and meteorological elements shown in ~~Fig.~~F~~f~~igure 3, the obvious positive correlations to surface air temperature and relative humidity, as well as a pronounced negative correlation to surface air pressure and a weak positive correlation to near-surface wind speed were found with the change of $PM_{2.5}$ concentrations in January 2016 (Table 1). The near-surface wind speed associated with East

Asian monsoons has significantly influence concentrations of air pollutants mainly by the changes in weak advection of cold air, in conjunction with strong subsidence and stable atmospheric stratification, can easily produce a stagnation area in the lower troposphere resulting in regional pollutant accumulations, which are favorable for the development of CEC haze events. In addition, in the presence of high soil moisture, strong surface evaporation results in increases in the near-surface relative humidity, which is also conducive to hygroscopic growth of participles for haze formation; high air temperature and strong solar radiation could enhance chemical reactions and conversions for the formation of secondary aerosols in the atmosphere, precipitation could alter the emissions, and depositions of air pollutants. These observations could reflect the special influences of meteorological factors (winds, air temperature, humidity, precipitation etc) on physical and chemical processes in the ambient atmosphere, in particular that of wind driving air pollutant transport and affecting air quality change in the YRMB region.

~~These observations could reflect the special influences of meteorological factors on physical and chemical processes in the ambient atmosphere, in particular that of wind driving air pollutant transport and affecting air quality change in the YRMB region.~~

When we focused on the changes leading to excessive $PM_{2.5}$ levels during these heavy air pollution events, it is noteworthy that all three heavy pollution episodes P1, P2 and P3 were accompanied with strong near-surface wind speeds in the northerly direction, as well as evident turning points in prevailing conditions leading to falling surface air temperatures and increasing surface air pressure (noted as a rectangle with red dashed lines in ~~Fig~~Ffig.~~ure .~~3). The conditions observed during these three heavy pollution episodes reflect the typical meteorological characteristics of cold front activity over the East Asian monsoon region. The southward advance of a cold front could drive the regional transport of air pollutants over central-eastern China (Kang et al., 2019). Climatologically, a strong northerly wind, low air temperature and high air pressure are typical features of an incursion of cold air during East Asian winter monsoon season in central-eastern China, which could disperse air pollutants and improve air quality in the NCP region (Miao et al., 2018;Xu et al., 2016b). Compared to the meteorological conditions for stagnation with weak winds observed for heavy air pollution events in the major air pollution regions of central-eastern China (Huang et al., 2018;Ding et al., 2017), meteorological conditions with strong near-surface wind were anomalously accompanied with the intensification of $PM_{2.5}$ during heavy air pollution periods over the study area in the YRMB in January 2016 (Fig. 3). This could imply the importance of regional air pollutant transport in worsening air quality over the YRMB, driven by the strong northerly winds of the East Asian winter monsoon over China.

2.3 A unique "non-stagnation" meteorological condition for heavy $PM_{2.5}$ pollution

To further investigate the connection of meteorological elements in the near-surface layer with changes in air quality affected by $PM_{2.5}$ concentrations in the YRMB region, we carried out a more detailed correlation analysis of $PM_{2.5}$ concentrations in Wuhan with near-surface wind speed and air temperature and three different levels of $PM_{2.5}$ concentrations: clean air environment ($PM_{2.5}$ <75μg m^{-3}), light air pollution (75μg m^{-3} ≤ $PM_{2.5}$ <150μg m^{-3}) and heavy air pollution ($PM_{2.5}$ ≥150μg m^{-3}) periods (Table 2). As seen in Table 2, the surface $PM_{2.5}$ concentrations were positively correlated with air temperature, as well as negatively correlated with wind speeds during the periods of clean air environment and light air pollution. It should be emphasized here that a significantly negative correlation (R=-0.19) of $PM_{2.5}$ concentrations with near-surface wind speeds for the light air pollution period could indicate that weak winds are favorable for local $PM_{2.5}$ accumulation, reflecting an important effect of local air pollutant emissions on light air pollution periods over the YRMB area. In January 2016, the overall wind speed of Wuhan was weak with a monthly mean value of 2.0 m s^{-1}, which could prove beneficial to maintaining the high $PM_{2.5}$ levels in the prolonged air pollution event experienced during January 2016. However, a significantly positive correlation (R=0.41) existed between excessive $PM_{2.5}$ concentrations ($PM_{2.5}$ > 150μg m^{-3}) and strong near-surface wind speeds during the heavy air pollution period, which was inconsistent with the stagnation meteorological conditions observed in the near-surface layer with weak winds associated with heavy air pollution in eastern China (Cao et al., 2012; Zhang et al., 2016). The meteorology and environment conditions in the YRMB region indicate the close association of heavy air pollution periods with the intensification of regional transport of air pollutants driven by strong winds (Fig. 3, Table 2) reflecting a key role of regional air pollutant transport in the development of the YRMB's heavy air pollution periods. ~~The conditions in the YRMB region that indicate that the close association of heavy air pollution periods with the intensification of regional transport of air pollutants by strong winds (Fig. 3, Table 2), which might reflect a key role of regional air pollutant transport in the development of the YRMB's heavy air pollution periods.~~

In order to clearly illustrate the impact of wind speed and direction on the $PM_{2.5}$ concentrations associated with the regional transport of upwind air pollutants, ~~Fig.~~Figure 4 presents the relation of hourly changes in surface $PM_{2.5}$ concentrations (in color contours) to near-surface wind speed (in radius of round) and direction (in angles of round) in Wuhan during January 2016. As can be seen in ~~Fig.~~Figure 4, strong northerly winds of the East Asian winter monsoon accompanied extremely high $PM_{2.5}$ concentrations (>150µg ~~µg~~ m^{-3}) during heavy air pollution periods, including the northeast gale that exceeded 5 $m{\cdot}s^{-1}$ during the extreme heavy pollution period with excessive high $PM_{2.5}$ concentrations (>300µg ~~µg~~ m^{-3}) over the YRMB region. These results reveal a unique meteorological condition of “non-stagnation” with strong winds during events of heavy air pollution over YRMB area. Conversely, the observed $PM_{2.5}$ concentrations~~,~~ ranging between 75 and 150 µg~~µg~~ m^{-3}~~,~~ for light air pollution periods generally corresponded with low wind speed (<2m s^{-1}) in the YRMB region (Fig. 4); therefore, it is the meteorological condition for stagnation characterized by weak winds involved in the accumulation of local air pollutants that is responsible for the YRMB’s light air pollution periods. Meteorological impacts on air quality could include not only the stagnation condition with weak winds and stable boundary layer, but also air temperature, humidity, precipitation, atmospheric radiation etc. in close connection with atmospheric physical and chemical processes. Therefore, meteorological drivers of air quality change are complicated by a series of physical and chemical processes in the atmosphere ~~Meteorological impacts that drive change in air quality are complicated by a series of physical and chemical processes in the atmosphere,~~ especially the formation of secondary air pollutants in the ~~wet~~ humid air environment ~~underlying~~ overlying the dense water network in the YRMB region (see ~~right panel of~~ Fig. 1b), thus pointing out the need for further comprehensive study.

As shown in ~~Fig~~Figure~~.~~ 2a, the heavy pollution periods with the daily average $PM_{2.5}$ concentrations exceeding 150µgm^{-3} in ambient air, respectively occurred on January 4, 10-12 and 18, and the clean air periods with the daily average $PM_{2.5}$ concentrations below 75µgm^{-3} occurred on January 22 and 24-27, 2016, in the YRMB region. The air sounding data of Wuhan were used to compare the structures of the atmospheric boundary layer of the heavy air pollution and clean air periods. ~~Fig.~~Figure 5 presents the vertical profiles of air temperature, wind velocity and potential temperature averaged for the heavy $PM_{2.5}$ pollution and clean air periods in January 2016. It can be clearly seen that the inversion layer of air temperature did not exist during the heavy pollution periods, but a near-surface inversion layer appeared at the height of about 200 m during the clean air periods (Fig. 5a). The comparison of vertical profiles of horizontal wind velocity experienced during the clean air periods further revealed the stronger wind speed observed in the heavy air pollution period below a height of 850 m located in the atmospheric boundary layer exhibiting the vertical structure similar to a low-level jet stream (Fig. 5b); these conditions could conduce the downward mixing of the regionally transported air pollutants and produce a local near-surface accumulation in the YRMB area with elevated ambient $PM_{2.5}$ concentrations, thus contributing to a heavy air pollution~~affecting a heavy air pollution period~~. To characterize the atmospheric stability in the boundary layer, the vertical profiles of potential air temperature (θ) were calculated with air temperature and pressure (Fig. 5c). The vertical change rate of θ was used to quantify the static stability of the boundary layer in this study (Oke, 2002;Sheng et al., 2003). A lower vertical change rate of θ generally indicates a decreasing stability or increasing instability of the boundary layer. The averaged static stability values of the near-surface layer below a height of 200 m during the heavy pollution and clean air periods were approximately 4.4~~-~~K·km^{-1} and 13.2K km^{-1}, respectively (Table 3). This obvious decrease in stability of the boundary layer from clean air to heavy pollution periods reflects an anomalous tendency for instability in the boundary layer during heavy pollution periods in the YRMB region during January 2016.

The meteorological conditions of stagnation characterized by weak wind, temperature inversion and a stable vertical structure of the atmospheric boundary layer is generally accepted as the typical meteorological drivers for heavy air pollution (An et al., 2019;Ding et al., 2017). Nevertheless, this study of environmental and meteorological observations in the YRMB region has revealed a unique meteorological condition of “non-stagnation” in the atmospheric boundary layer during heavy air pollution periods characterized by strong wind, lack of an inversion layer and a more unstable structure of the atmospheric boundary layer; these conditions are generally regarded as the typical pattern of atmospheric circulation that facilitates the regional transport of air pollutants from upstream source to downwind receptor regions. Regional ~~$PM_{2.5}$~~ transport of $PM_{2.5}$ associated with the source-receptor relationship between the air pollution regions in central-eastern China and the YRMB was investigated based on the observational analysis described in Sect. 3.1.

3. Regional transport of $PM_{2.5}$ in heavy air pollution periods

3.1 Changes of $PM_{2.5}$ and winds observed in central-eastern China

The monthly averages of observed $PM_{2.5}$ concentrations and the anomalies of wind speed averaged in three heavy air pollution periods relatively to the monthly mean wind speed in January 2016 over central-eastern China are shown in ~~Fig~~fFigure~~.~~ 6. In January 2016, a large area of central-eastern China experienced air pollution with high levels of $PM_{2.5}$ (>75 μg m^{-3}), especially serious in the NCP region and the Fenhe-Weihe Plain in central China (Fig. 6a). As seen in fFigure~~Fig.~~ 6, the YRMB region (Site 1, Wuhan) was situated in the downwind southern edge of an observed air pollution area located over central-eastern China, where the northerly winds of the East Asian winter monsoon prevail climatologically in January (Ding, 1994). It is notable that the anomalously stronger northerly winds were observed over the upstream region in central-eastern

China during three periods of wintertime heavy $PM_{2.5}$ pollution in the YRMB region (Fig. 6b). Driven by the strong northerly winter monsoonal winds (Fig. 6b), the regional transport of air pollutants from the source regions in central-eastern China could largely contribute to wintertime heavy air pollution periods in the downwind receptor region of YRMB.

In order to explore the connection of regional ~~$PM_{2.5}$~~ transport of $PM_{2.5}$ over central-eastern China to three events of heavy air pollution in the YRMB region, six observational sites were selected from the northwestern, northern and northeastern upwind areas located over central-eastern China (Fig. 6a) to represent the temporal $PM_{2.5}$ and wind variations along the different routes of regional ~~$PM_{2.5}$~~ transport of $PM_{2.5}$ with the southward incursion of stronger northerly winds of East Asian monsoon across central-eastern China (Fig. 7). The southeastward movement of heavy $PM_{2.5}$ pollution driven by stronger northerly winds from Luoyang and Xinyang to Wuhan (Sites 3, 2, and 1 in Fig. 6) presents a northwestern route of regional ~~$PM_{2.5}$~~ transport of $PM_{2.5}$ for the heavy air pollution period P1 in the YRMB (see upper panels of Fig. 7). The southwestward advance of $PM_{2.5}$ peaks governed by winter monsoonal winds the from Tongling and Hefei to Wuhan (Sites 5, 6, and 1 in Fig. 6) exerted a significant impact on the heavy air pollution period P2 aggravated by regional transport of $PM_{2.5}$ across Eastern China to the YRMB region (see middle panels of Fig. 7). A northern pathway of regional ~~$PM_{2.5}$~~ transport of $PM_{2.5}$ connected Zhengzhou and Xinyang to Wuhan (Sites 4, 2, and 1 in Fig. 6) during the YRMB's heavy air pollution period P3 with anomalously strong northerly winds (see Fig. 6b and lower panels of Fig. 7). It is noteworthy in Fig. 7 that the heavy $PM_{2.5}$ pollution periods at the upstream sites Hefei, Tongling, Luoyang, Xinyang and Zhengzhou (Fig. 6a) were generally dispelled by strong northerly winds, while strong northerly winds could trigger the periods of heavy $PM_{2.5}$ pollution in the YRMB region (Wuhan, Fig. 6), and such inverse effects of strong winds on heavy air pollution in the source and receptor regions reflect an important role of regional air pollutant transport in worsening air pollution in the YRMB's receptor region.

The regional ~~$PM_{2.5}$~~ transport over central-eastern China associated with the source-receptor relationship directing heavy $PM_{2.5}$ pollution to the YRMB region was revealed with observational analysis. Backward trajectory modeling was used to further confirm the patterns of regional ~~$PM_{2.5}$~~ transport of $PM_{2.5}$ over central-eastern China and the resulting contribution to heavy air pollution in the YRMB region, as described in the following Sects.

3.2 FLEXPART-WRF model

3.2.1 Model description

The Flexible Particle dispersion (FLEXPART) model (Stohl, 2003) is a Lagrange particle diffusion model developed by the Norwegian Institute for Air Research (NIAR). In this model, the trajectory of a large number of particles released from a source is ~~simulated~~ simulated with consideration of the processes of tracer transport, turbulent diffusion, and wet and dry depositions in the atmosphere (Brioude et al., 2013). Applying backward trajectory simulation can determine the distribution of potential source regions that may have an impact on a target point or receptor region (Seibert and Frank, 2003;Zhai et al., 2016;Chen et al., 2017a; Chen et al., 2017b).

Initially, FLEXPART could be driven by the global reanalysis meteorological data obtained from the European Centre for Medium-Range Weather Forecasts (ECMWF) or the National Centers of Environmental Prediction (NCEP). For the refined simulation of air pollutant sources and transport, FLEXPART was coupled offline with the Weather Research and Forecasting Model

(WRF) to effectively devise the combined model FLEXPART-WRF (Fast and Easter, 2006), which has been widely used to investigate the potential sources of air pollutants in consideration of environmental change (Stohl, 2003;De Foy et al., 2011;An et al., 2014;Sauvage et al., 2017).

3.2.2 Model configuration

The WRF model was configured with two nested domains. The coarse domain covered the entirety of Asia with a 30 km×30 km horizontal resolution, and the nested fine domain included most of China and surrounding regions with a 10 km×10 km horizontal resolution. The physical parameterizations used in WRF were selected with the Morrison microphysics scheme (Morrison, 2009), the Rapid Radiative Transfer Model (RRTM) scheme for long and short wave radiation (Mlawer et al., 1997), the Yonsei University (YSU) boundary layer scheme (Hong, 2006), Grell 3D cumulus parameterization, and the Noah land surface scheme (Grell et al., 2005). Driven with the reanalysis meteorological data obtained from NCEP for initial and boundary meteorological conditions, the WRF simulation ran 12 h each time with the first 6 h simulations constituting spin-up time.

The FLEXPART-WRF simulation was conducted for the 48-hr backward trajectory with a release of 50,000 $PM_{2.5}$ particles per hour in Wuhan (30.61N, 114.42E) for January 2016. The 48-hr backward trajectory simulation results were output with the residence time of $PM_{2.5}$ particles in a horizontally resolution of 0.1°×0.1°. The FLEXPART simulations of $PM_{2.5}$ particle residence time over the 48-hr backward trajectory pathways were multiplied with the regional primary $PM_{2.5}$ emission fluxes to quantify the contribution of regional ~~$PM_{2.5}$~~ transport of $PM_{2.5}$ to air quality change in the YRMB region with identifying the patterns of regional ~~$PM_{2.5}$~~ transport of $PM_{2.5}$

~~patterns~~ over central-eastern China. The primary $PM_{2.5}$ emission data of 2016 obtained from the Multi-resolution Emission Inventory for China (MEIC, http://www.meicmodel.org/) were selected for use as the regional $PM_{2.5}$ emission fluxes in this study.

3.2.3 Validation of ~~M~~modeling ~~R~~results ~~Modeling Validations~~

The simulated meteorology, which included wind speed, air temperature, relative humidity and surface pressure, were compared with observations at five sites (Wuhan, Changsha, Hefei, Zhengzhou and Nanchang) over central-eastern China. The correlation coefficients and normalized standardized deviations were calculated and are shown in ~~f~~Figure~~Fig.~~ 8 (Taylor, 2001). Based on the results with correlation coefficients passing the significance level of 0.001 and low normalized standardized deviations (Fig. 8), it was confirmed that WRF-modeled meteorology that is consistent with observations could be used to drive the FLEXPART backward trajectory simulation in this study.

3.3 Contribution of regional ~~$PM_{2.5}$~~ transport of $PM_{2.5}$ to heavy pollution

Based on the FLEXPART-WRF backward trajectory simulation, the upstream sources of $PM_{2.5}$ emissions for heavy air pollution in Wuhan could be identified. The contribution rates $\boldsymbol{rate_{i,j}}$ of regional ~~$PM_{2.5}$~~ transport of $PM_{2.5}$ from the upstream sources to air pollution in the downstream receptor region of YRMB were calculated by Eq. (1), and the total contribution $\boldsymbol{R}$ of regional transport from the non-local emission sources are estimated by Eq. (2) (Chen et al., 2017b).

$$rate_{i,j} = \frac{E_{i,j} \times r_{i,j}}{\sum_{1,1}^{N,S} E_{i,j} \times r_{i,j}} \qquad (1)$$

$$R = \sum_{(N_1,S_1)}^{(N_2,S_2)} rate_{i,j} \qquad (2)$$

where the subscripts $\boldsymbol{i}$ and $\mathbf{j}$ represent a grid location; $\mathbf{r}_{i,j}$ represents the residence time of $PM_{2.5}$ particles simulated by FLEXPART-WRF; and, $E_{i,j}$ represents the $PM_{2.5}$ emission flux over the grid. The first grid location (N_1, S_1) and the last grid location (N_2, S_2) over the non-local emission sources and the local area of Wuhan were determined respectively by the regional ~~$PM_{2.5}$~~ transport of $PM_{2.5}$ pathways and the YRMB region as simulated by FLEXPART-WRF.

The non-local emission sources that affected $PM_{2.5}$ concentrations during three heavy pollution periods through regional transport to the YRMB region were quantified by calculation of the $PM_{2.5}$ contribution rates with Eq (1). Combining the distribution of high $PM_{2.5}$ contribution rates with the prevailing winds experienced during the three heavy $PM_{2.5}$ pollution periods, the spatial distribution of the major pathways of regional ~~$PM_{2.5}$~~ transport of $PM_{2.5}$ over central-eastern China could be recognized as shown in ~~f~~Figure~~Fig.~~ 9. During the heavy air pollution period P1 in the YRMB region, the regional transport of air pollutants was centered along a northwestern route from the Fenhe-Weihe Plain in central China and a northeastern route from the YRD region (Fig. 9a). The YRD emission sources of air pollutants in East China exerted an important impact on the heavy air pollution period P2 through regional ~~$PM_{2.5}$~~ transport of $PM_{2.5}$ cross East China to the YRMB region along the north side of Yangtze River (Fig. 9b). Two major regional transport pathways of $PM_{2.5}$ indicated by the spatial distribution of high contribution rates of $PM_{2.5}$ from the NCP and YRD regions respectively to the elevated $PM_{2.5}$ concentrations during the YRMB's heavy air pollution period P3 (Fig. 9c). ~~Two major pathways of regional $PM_{2.5}$ transport of $PM_{2.5}$~~

~~connected high contribution rates of air pollutants from the NCP and YRD regions, respectively, to the elevated $PM_{2.5}$ concentrations that characterized the YRMB's heavy air pollution period P3 (Fig. 9c).~~ Governed by the northerly winds of the East Asian winter monsoon, the regional transport of air pollutants from the central-eastern air pollutant emission source regions in China provided a significant contribution to the wintertime heavy $PM_{2.5}$ pollution observed in the YRMB region (Figs. 6-7), which was confirmed by the results of the FLEXPART-WRF backward trajectory simulation utilized in this study.

In this study, the $PM_{2.5}$ contributions of regional transport to air pollution in the downwind receptor region could be approximately estimated based on the product of the residence time of $PM_{2.5}$ particles during regional transport simulated by FLEXPART-WRF, and the $PM_{2.5}$ emission flux over the source grid. The $PM_{2.5}$ contributions of regional transport over central-eastern China to $PM_{2.5}$ concentrations during three heavy $PM_{2.5}$ pollution periods P1, P2 and P3 in the YRMB region were estimated using Eq. (2) with resulting high contribution rates of 68.1%, 60.9%and 65.3%, respectively (Table 4), revealing the significant contribution of regional transport of $PM_{2.5}$ over central-eastern China to the enhancement of $PM_{2.5}$ levels in the YRMB area during wintertime heavy air pollution periods.

~~The relative contributions of regional $PM_{2.5}$ transport of $PM_{2.5}$ over central-eastern China to the three heavy $PM_{2.5}$ pollution periods P1, P2 and P3 in the YRMB region were estimated using Eq. (2) with resulting high contribution rates of 68.1%, 60.9% and 65.3%, respectively (Table 4), revealing the significant contribution of regional $PM_{2.5}$ transport of $PM_{2.5}$ over central-eastern China to the enhancement of $PM_{2.5}$ levels in the YRMB area during the heavy air pollution periods accompanied by the unique "non-stagnation" meteorological conditions in the~~

~~atmospheric boundary layer.~~

Normally people rely on 3-D numerical models with process analysis capability such as integrated process rates (IPRs) to quantify the contributions of regional transport to the occurrence of air pollution episodes. It should be pointed out that the simulations with a Lagrange particle dispersion model FLEXPART-WRF are utilized to calculate the percentage contribution of regional transport with identifying the transport pathway in this study. The major uncertainty of this method for such calculation as compared to other methods like IPRs is that the physical and chemical processes such as wet-deposition and chemical conversion for the formation of secondary particles are not introduced in the FLEXPART-WRF simulation, which could represent the basic features of contribution and patterns of regional ~~$PM_{2.5}$~~ transport of $PM_{2.5}$ over central-eastern China when limited to the primary $PM_{2.5}$ particles highlighted in this study.

4. Conclusions

This study investigated the ambient $PM_{2.5}$ variations over Wuhan, a typical urban YRMB region in central-eastern China in January 2016 through analysis of observational data of environment and meteorology, as well as via FLEXPART-WRF simulation to explore 1) the meteorological processes involved in the regional transport of air pollutants and 2) regional transport patterns of $PM_{2.5}$ with the contribution to the air pollution in the YRMB region. Based on observation and simulation studies on the meteorological conditions of air pollution events in January 2016 and regional transport of $PM_{2.5}$ to heavy air pollution over the YRMB region, it is revealed heavy air pollution with the unique "non-stagnant" atmospheric boundary layer in the YRMB region aggravated by regional transport of $PM_{2.5}$ over central and eastern China.

The study of the effects of meteorology and regional transport of $PM_{2.5}$ on heavy air pollution were focused on three heavy $PM_{2.5}$ pollution periods in January 2016. The heavy pollution episodes observed with the peak of $PM_{2.5}$ concentrations exceeding 471μg m^{-3} over the YRMB region were characterized by a short duration of less than 26 hr from rapid outbreak to fast dissipation.

~~This study investigated the ambient $PM_{2.5}$ variations over Wuhan, a typical urban YRMB region in central-eastern China in January 2016 through analysis of observational data of environment and meteorology, as well as via FLEXPART-WRF simulation. Study of the effects of meteorology and regional transport of air pollutant on periods of heavy air pollution were focused on three observed heavy pollution events in January 2016 with $PM_{2.5}$ peak concentrations exceeding 471 μg m^{-3}. The heavy pollution episodes over the YRMB region were characterized by a short duration of less than 26 hr from rapid outbreak to fast dissipation.~~

The “stagnation” meteorological condition in the boundary layer characterized by weak wind, air temperature inversion and a stable vertical structure of the atmospheric boundary layer is currently accepted as a typical meteorological driver for heavy air pollution. Conversely, this study of environmental and meteorological observations in the YRMB region revealed a unique “non-stagnation” meteorological condition of the boundary layer characterized by strong wind, no inversion layer and a more unstable structure in the atmospheric boundary layer associated with heavy air pollution periods with excessive $PM_{2.5}$ concentrations in the YRMB region, which facilitates understanding of the air pollutant source-receptor relationship of regional air pollutant transport.

Although the emissions and local accumulation of air pollutants in the YRMB could lead to the formation of light air pollution, in regards to $PM_{2.5}$, over the YRMB region, the regional ~~$PM_{2.5}$~~ transport of $PM_{2.5}$ from central-eastern emission source regions in China contributed significantly to 65% of the exceedances of $PM_{2.5}$ concentrations during wintertime heavy air pollution periods in the downwind YRMB region in January 2016, as governed by the strong northerly winds of the East Asian winter monsoon.

Based on the variations of air quality and meteorology in a typical urban YRMB region in January 2016, this study revealed a unique “non-stagnant” meteorological condition for the development of heavy air pollution in the YRMB region with strong contributions of regional ~~$PM_{2.5}$~~ transport of $PM_{2.5}$ over central-eastern China. These conditions and contributions can be investigated further with climate analyses of long-term observations and a more comprehensive modeling of air quality and meteorology.

Data availability: Data used in this paper can be provided by Chao Yu (ychao012@foxmail.com) upon request.

Author contributions: CY, TZ and YB conducted the study design. XY, LZ and SK provided the observational data. LZ assisted with data processing. CY wrote the manuscript with the help of TZ and XY. YB, SK, JH, CC, YY, GM, MW and JC were involved in the scientific interpretation and discussion. All of the authors provided commentary on the paper.

Competing interests: The authors declare that they have no conflicts of interest.

Acknowledgement: This study was jointly funded by the National Natural Science Foundation of

China (41830965; 91744209), the National Key R & D Program Pilot Projects of China (2016YFC0203304) and the Postgraduate Research & Practice Innovation Program of Jiangsu Province (KYCX18_1027).

Reference

Acciai, C., Zhang, Z., Wang, F., Zhong, Z., and Lonati, G.: Characteristics and source Analysis of trace Elements in PM2.5 in the Urban Atmosphere of Wuhan in Spring, Aerosol and Air Quality Research, 17, https://doi.org/2224-2234, 10.4209/aaqr.2017.06.0207, 2017.

An, X., Yao, B., Li, Y., Li, N., and Zhou, L.: Tracking source area of Shangdianzi station using Lagrangian particle dispersion model of FLEXPART, Meteorological Applications, 21, 466-473, https://doi.org/10.1002/met.1358, 2014.

An, Z., Huang, R.-J., Zhang, R., Tie, X., Li, G., Cao, J., Zhou, W., Shi, Z., Han, Y., and Gu, Z.: Severe haze in Northern China: A synergy of anthropogenic emissions and atmospheric processes, Proceedings of the National Academy of Sciences, 116, 8657-8666, https://doi.org/10.1073/pnas.1900125116 ,2019.

Brioude, J., Arnold, D., Stohl, A., Cassiani, M., Morton, D., Seibert, P., Angevine, W., Evan, S., Dingwell, A., Fast, J. D., Easter, R. C., Pisso, I., Burkhart, J., and Wotawa, G.: The Lagrangian particle dispersion model FLEXPART-WRF version 3.1, Geoscientific Model Development, 6, 1889-1904, https://doi.org/10.5194/gmd-6-1889-2013, 2013.

Cao, J. J., Wang, Q. Y., Chow, J. C., Watson, J. G., Tie, X. X., Shen, Z. X., Wang, P., and An, Z. s.: Impacts of aerosol compositions on visibility impairment in Xi'an, China, Atmospheric

Environment, 59, 559-566, https://doi.org/10.1016/j.atmosenv.2012.05.036, 2012.

Chang, X., Wang, S., Zhao, B., Cai, S., and Hao, J.: Assessment of inter-city transport of particulate matter in the Beijing–Tianjin–Hebei region, Atmospheric Chemistry and Physics, 18, 4843-4858, https://doi.org/10.5194/acp-18-4843-2018, 2018.

Chen, B., Xu, X.-D., and Zhao, T.: Quantifying oceanic moisture exports to mainland China in association with summer precipitation, Climate Dynamics, 1-16, https://doi.org/10.1007/s00382-017-3925-1 ,2017a.

Chen, S., Zhou, G., Zhu, B., Geng, F., and Chang, L.: A method for fast quantification of air pollutant sources, Acta Scientiae Circumstantiae, 2474-2481, 2017b.

Cheng, Y. F., Wiedensohler, A., Eichler, H., Heintzenberg, J., Tesche, M., Ansmann, A., Wendisch, M., Su, H., Althausen, D., and Herrmann, H.: Relative humidity dependence of aerosol optical properties and direct radiative forcing in the surface boundary layer at Xinken in Pearl River Delta of China: An observation based numerical study, Atmospheric Environment, 42, 6373-6397, https://doi.org/10.1016/j.atmosenv.2008.04.009, 2008.

De Foy, B., Burton, S. P., Ferrare, R. A., Hostetler, C. A., Hair, J. W., Wiedinmyer, C., and Molina, L. T.: Aerosol plume transport and transformation in high spectral resolution lidar measurements and WRF-Flexpart simulations during the MILAGRO Field Campaign, Atmospheric Chemistry and Physics, 11, 3543-3563, https://doi.org/10.5194/acp-11-3543-2011, 2011.

Deng, J., Wang, T., Jiang, Z., Xie, M., Zhang, R., Huang, X., and Zhu, J.: Characterization of visibility and its affecting factors over Nanjing, China, Atmospheric Research, 101, 681-691, https://doi.org/10.1016/j.atmosres.2011.04.016, 2011.

Ding, Y. H.: Monsoons over China, Kluwer Academic Publishers, Dordrecht/Boston/London, 1994.

Ding, Y., Wu, P., Liu, Y., and Song, Y.: Environmental and dynamic conditions for the occurrence of persistent haze events in north China, Engineering, 3, 266-271, 2017.

Fast, J. D., and Easter, R. C.: A Lagrangian particle dispersion model compatible with WRF, 7th Annual WRF User's Workshop, 2006, 19-22.

Fuzzi, S., Baltensperger, U., Carslaw, K., Decesari, S., Denier van der Gon, H., Facchini, M. C., Fowler, D., Koren, I., Langford, B., and Lohmann, U.: Particulate matter, air quality and climate: lessons learned and future needs, Atmospheric chemistry and physics, 15, 8217-8299, https://doi.org/10.5194/acp-15-8217-2015,2015.

Gong, W., Zhang, T., Zhu, Z., Ma, Y., Ma, X., and Wang, W.: Characteristics of PM1.0, PM2.5, and PM10, and Their Relation to Black Carbon in Wuhan, Central China, Atmosphere, 6, 1377-1387, https://doi.org/10.3390/atmos6091377, 2015.

Grell, G. A., Peckham, S. E., Schmitz, R., McKeen, S. A., Frost, G., Skamarock, W. C., & Eder, B. ~~Grell G A, Schmitz P R, Mckeen S A, et al~~. Fully coupled 'online' chemistry within the WRF model~~[J]~~. Atmospheric Environment, ~~,~~ 39(37):6957-~~6975~~ 6975, https://doi.org/10.1016/j.atmosenv.2005.04.027, 2005.

He, J., Mao, H., Gong, S., Yu, Y., Wu, L., Liu, H., Chen, Y., Jing, B., Ren, P., and Zou, C.: Investigation of Particulate Matter Regional Transport in Beijing Based on Numerical Simulation, Aerosol and Air Quality Research, 17, 1181-1189, https://doi.org/10.4209/aaqr.2016.03.0110, 2017.

Hong S Y, Noh Y, Dudhia J. ~~Hong, S. Y.~~: A new vertical diffusion package with an explicit treatment of entrainment processes, Monthly Weather Review, 134, 2318-2341, https://doi.org/10.1175/MWR3199.1,2006.

Hu, J., Li, Y., Zhao, T., Liu, J., Hu, X.-M., Liu, D., Jiang, Y., Xu, J., and Chang, L.: An important mechanism of regional O_3 transport for summer smog over the Yangtze River Delta in eastern China, Atmospheric Chemistry and Physics, 18, 16239-16251, https://doi.org/10.5194/acp-18-16239-2018 ,2018.

Huang, Q., Cai, X., Wang, J., Song, Y., and Zhu, T.: Climatological study of the Boundary-layer air Stagnation Index for China and its relationship with air pollution, Atmos. Chem. Phys., 18, 7573–7593, https://doi.org/10.5194/acp-18-7573-2018, 2018.

Jiang, C., Wang, H., Zhao, T., Li, T., and Che, H.: Modeling study of PM2.5 pollutant transport across cities in China's Jing–Jin–Ji region during a severe haze episode in December 2013, Atmospheric Chemistry and Physics, 15, 5803-5814, https://doi.org/10.5194/acp-15-5803-2015, 2015.

Kan, H., Chen, R., and Tong, S.: Ambient air pollution, climate change, and population health in China, Environment international, 42, 10-19, https://doi.org/10.1016/j.envint.2011.03.003, 2012.

Kang, H., Zhu, B., Gao, J., He, Y., Wang, H., Su, J., Pan, C., Zhu, T., and Yu, B.: Potential impacts of cold frontal passage on air quality over the Yangtze River Delta, China, Atmospheric Chemistry and Physics, 19, 3673-3685, https://doi.org/10.5194/acp-19-3673-2019, 2019.

Miao, Y., Guo, J., Liu, S., Zhao, C., Li, X., Zhang, G., Wei, W., and Ma, Y.: Impacts of synoptic condition and planetary boundary layer structure on the trans-boundary aerosol transport from Beijing-Tianjin-Hebei region to northeast China, Atmospheric Environment, 181, 1-11, https://doi.org/10.1016/j.atmosenv.2018.03.005, 2018.

Mlawer, E. J., Taubman, S. J., Brown, P. D., Iacono, M. J., and Clough, S. A.: Radiative transfer for inhomogeneous atmospheres: RRTM, a validated correlated-k model for the longwave, Journal of Geophysical Research: Atmospheres, 102, 16663-16682, https://doi.org/10.1029/97jd00237, 1997.

Morrison, H.: Impact of cloud microphysics on the development of trailing stratiform precipitation in a simulated squall ~~line:Comparison~~line: Comparison of one-and two-moment schemes, Mon.wea.rev, 137, 991-1007, https://doi.org/10.1175/2008MWR2556.1, 2009.

Nel, A.: Air pollution-related illness: effects of particles, Science, 308, 804-806, https://doi.org/10.1126/science.1108752, 2005.

Oke, T. R.: Boundary layer climates, Routledge, 2002.

Qiao, X., Guo, H., Tang, Y., Wang, P., Deng, W., Zhao, X., Hu, J., Ying, Q., and Zhang, H.: Local and regional contributions to fine particulate matter in the 18 cities of Sichuan Basin, southwestern China, Atmos. Chem. Phys., 19, 5791–5803, https://doi.org/10.5194/acp-19-5791-2019, 2019.

Sauvage, B., Fontaine, A., Eckhardt, S., Auby, A., Boulanger, D., Petetin, H., Paugam, R., Athier, G., Cousin, J.-M., Darras, S., Nédélec, P., Stohl, A., Turquety, S., Cammas, J.-P., and Thouret, V.: Source attribution using FLEXPART and carbon monoxide emission inventories: SOFT-IO version 1.0, Atmospheric Chemistry and Physics, 17, 15271-15292, https://doi.org/10.5194/acp-17-15271-2017, 2017.

Seibert, P., and Frank, A.: Source-receptor matrix calculation with a Lagrangian particle dispersion model in backward mode, Atmospheric Chemistry and Physics, 51-63, https://doi.org/10.5194/acp-4-51-2004, 2003.

Sheng, P., Mao, J., and Li, J.: Atmospheric physics, Peking University Press, 2003.

Stohl, A.: A backward modeling study of intercontinental pollution transport using aircraft measurements, Journal of Geophysical Research, 108, 1-8, https://doi.org/10.1029/2002jd002862, 2003.

Tan, C. H., Zhao, T. L., Cui, C. G., Luo, B. L., Zhang, L., and Bai, Y. Q.: Characterization of haze pollution over Central China during the past 50 years, China Environmental Science, 35, 2272-2280, 2015.

Taylor, K. E.: Summarizing multiple aspects of model performance in a single diagram, Journal of Geophysical Research Atmospheres, 106, 7183-7192, https://doi.org/10.1029/2000JD900719, 2001.

Tie, X., Huang, R. J., Cao, J., Zhang, Q., Cheng, Y., Su, H., Chang, D., Poschl, U., Hoffmann, T., Dusek, U., Li, G., Worsnop, D. R., and O'Dowd, C. D.: Severe Pollution in China Amplified by Atmospheric Moisture, Scientific reports, 7, 1-8, https://doi.org/10.1038/s41598-017-15909-1, 2017.

Wang, H. L., Qiao, L. P., Lou, S. R., Zhou, M., Ding, A. J., Huang, H. Y., Chen, J. M., Wang, Q., Tao, S. K., Chen, C. H., Li, L., and Huang, C.: Chemical composition of PM2.5 and meteorological impact among three years in urban Shanghai, China, Journal of Cleaner Production, 112, 1302-1311, https://doi.org/10.1016/j.jclepro.2015.04.099, 2016.

Wang, S. X., Zhao, B., Cai, S. Y., Klimont, Z., Nielsen, C. P., Morikawa, T., Woo, J. H., Kim, Y., Fu, X., Xu, J. Y., Hao, J. M., and He, K. B.: Emission trends and mitigation options for air pollutants in East Asia, Atmospheric Chemistry and Physics, 14, 6571-6603, https://doi.org/10.5194/acp-14-6571-2014, 2014.

Wu, J., Kong, S., Wu, F., Cheng, Y., Zheng, S., Yan, Q., Zheng, H., Yang, G., Zheng, M., and Liu, D.: Estimating the open biomass burning emissions in central and eastern China from 2003 to

2015 based on satellite observation, Atmospheric Chemistry & Physics, 18, https://doi.org/10.5194/acp-18-11623-2018, 2018.

Wu, P., Ding, Y., and Liu, Y.: Atmospheric Circulation and Dynamic Mechanism for Persistent Haze Events in the Beijing-Tianjin-Hebei Region, Advances in Atmospheric Sciences, 34, 429-440, 2017.

Xu, G., Jiao, L., Zhang, B., Zhao, S., Yuan, M., Gu, Y., Liu, J., and Tang, X.: Spatial and Temporal Variability of the PM2.5/PM10 Ratio in Wuhan, Central China, Aerosol and Air Quality Research, 17, 741-751, https://doi.org/10.4209/aaqr.2016.09.0406, 2017.

Xu, J., Chang, L., Qu, Y., Yan, F., Wang, F., and Fu, Q.: The meteorological modulation on PM2. 5 interannual oscillation during 2013 to 2015 in Shanghai, China, Science of The Total Environment, 572, 1138-1149, https://doi.org/10.1016/j.scitotenv.2016.08.024, 2016a.

Xu, X., Zhao, T., Liu, F., Gong, S. L., Kristovich, D., Lu, C., Guo, Y., Cheng, X., Wang, Y., and Ding, G.: Climate modulation of the Tibetan Plateau on haze in China, Atmospheric Chemistry and Physics, 16, 1365-1375, https://doi.org/10.5194/acp-16-1365-2016, 2016b.

Zhai, S., An, X., Liu, Z., Sun, Z., and Hou, Q.: Model assessment of atmospheric pollution control schemes for critical emission regions, Atmospheric Environment, 124, 367-377, https://doi.org/10.1016/j.atmosenv.2015.08.093, 2016.

Zhang, F., Wang, Z.-w., Cheng, H.-r., Lv, X.-p., Gong, W., Wang, X.-m., and Zhang, G.: Seasonal variations and chemical characteristics of PM2. 5 in Wuhan, central China, Science of the Total Environment, 518, 97-105, https://doi.org/10.1016/j.scitotenv.2015.02.054, 2015.

Zhang, H., Lv, M., and Zhang, B.: Analysis of the stagnant meteorological situation and the transmission condition of continuous heavy pollution course from February 20 to 26, 2014 in

Beijing-Tianjin-Hebei, Acta Scientiae Circumstantiae 36, 4340-4351, 2016.

Zhang, R., Li, Q., and Zhang, R.: Meteorological conditions for the persistent severe fog and haze event over eastern China in January 2013, Science China Earth Sciences, 57, 26-35, https://doi.org/10.1007/s11430-013-4774-3, 2014.

Zhang, X. Y., Wang, Y. Q., Niu, T., Zhang, X. C., Gong, S. L., Zhang, Y. M., and Sun, J. Y.: Atmospheric aerosol compositions in China: spatial/temporal variability, chemical signature, regional haze distribution and comparisons with global aerosols, Atmospheric Chemistry and Physics, 12, 779-799, https://doi.org/10.5194/acp-12-779-2012, 2012.

Zheng, H., Kong, S., Wu, F., Cheng, Y., Niu, Z., Zheng, S., Yang, G., Yao, L., Yan, Q., and Wu, J.: Intra-regional transport of black carbon between the south edge of the North China Plain and central China during winter haze episodes, Atmospheric Chemistry and Physics, 19, 4499-4516, https://doi.org/10.5194/acp-19-4499-2019, 2019.

Zhong, Zhangxiong, Huang, Zhen, Ting, Shen, and Longjiao: Characteristic Analysis of OC and EC in PM2.5 of Typical Haze Weather in Wuhan City, Meteorological and Environmental Research, 19-22, 2014.

Table 1. Correlation coefficients between hourly $PM_{2.5}$ concentrations and meteorological

elements over Wuhan in January 2016.

Correlation coefficient	WS	T	P	RH
$PM_{2.5}$	0.10	0.31	-0.47	0.20

Table 2. Correlation coefficients of $PM_{2.5}$ concentrations with wind speed and air temperature in different air quality levels during the study period.

Air quality	$PM_{2.5}$ levels	Number of samples	WS	T
Clean	$PM_{2.5} < 75 \mu g \cdot m^{-3}$	73	-0.20	0.56
Light pollution	$75 \mu g \cdot m^{-3} \leq PM_{2.5} < 150 \mu g \cdot m^{-3}$	135	-0.19	0.15
Heavy pollution	$PM_{2.5} \geq 150 \mu g \cdot m^{-3}$	37	0.41	-0.08

Table 3. Atmospheric static stability below heights of 200 m in the boundary layer during heavy pollution and clean air periods with the anomalies relative to the average over January, 2016 in Wuhan.

Period	heavy pollution period (K·km-1)	clean air period (K·km-1)	monthly average (K·km-1)
Static stability	4.4	13.2	8.6
Anomalies of stability	-4.2	4.6	-

Table 4. The relative contributions of regional ~~$PM_{2.5}$~~ transport over central-eastern China to three $PM_{2.5}$ heavy pollution periods P1, P2 and P3 in the YRMB with the local contributions.

Contribution rates	P1	P2	P3	Averages
Regional transport	68.1%	60.9%	65.3%	65.1%
Local contribution~~emissions~~	31.9%	39.1%	34.7%	34.9%

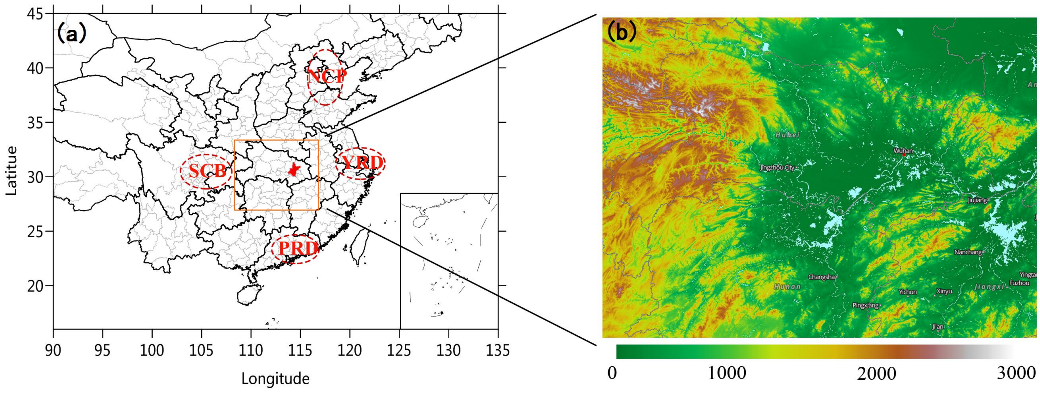

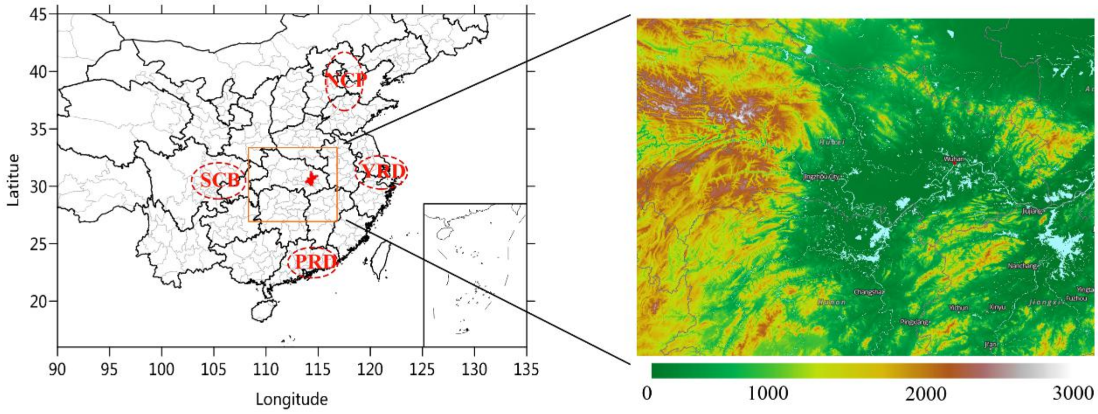

Fig. 1. (~~left panel~~a) Distribution of the Yangtze River Middle Basin (~~YRMB, ~~orange rectangle) with the location of Wuhan (red area) and the major haze pollution regions of NCP, YPD and SCB in central-eastern China as well as (~~right panle~~b) the YRMB region with terrain height (color contours, m in a.s.l.), the rivers~~,~~ and lake network (blue areas),downloaded from https://worldview.earthdata.nasa.gov.

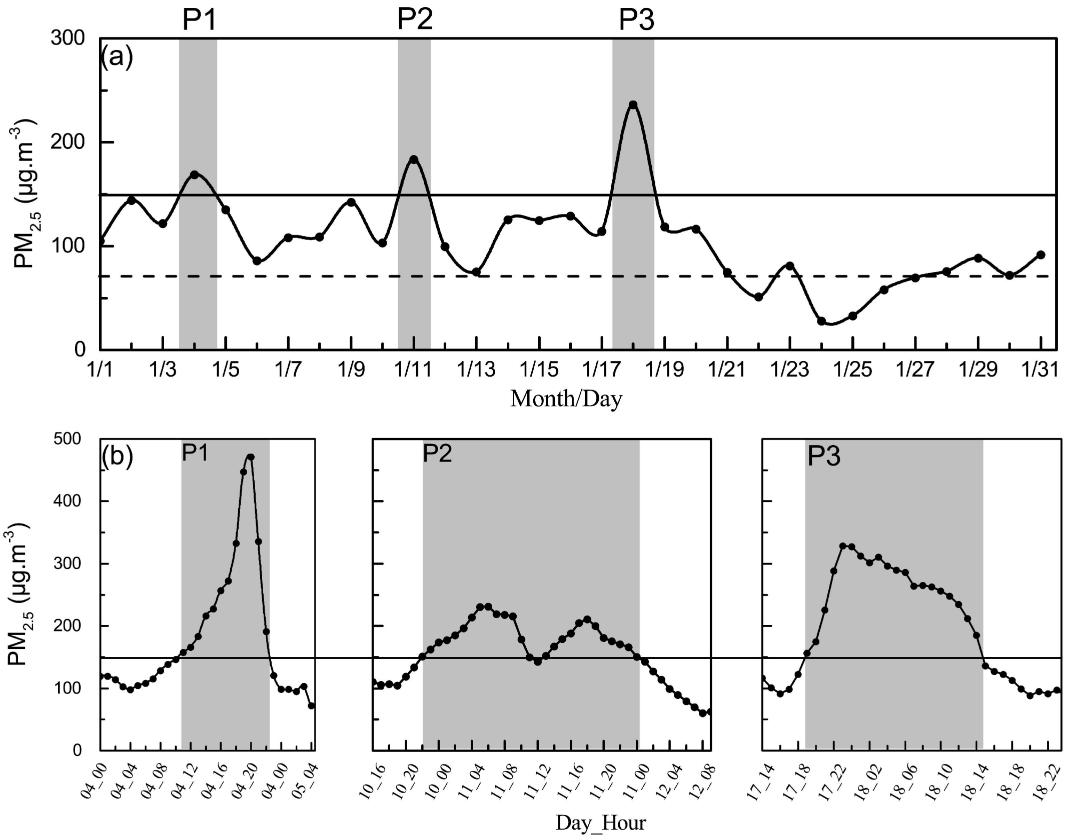

Fig. 2. (a) The daily changes of surface $PM_{2.5}$ concentrations in Wuhan in January 2016 with $PM_{2.5}$ concentrations exceeding 75 $\mu g \cdot m^{-3}$ (dash line) and 150 $\mu g \cdot m^{-3}$ (solid lines), respectively, for light and heavy haze pollution, and (b) the hourly variation of surface $PM_{2.5}$ concentrations in three heavy air pollution events P1, P2 and P3 with excessive $PM_{2.5}$ levels (>150 $\mu g\ m^{-3}$) marked by the shaded areas.

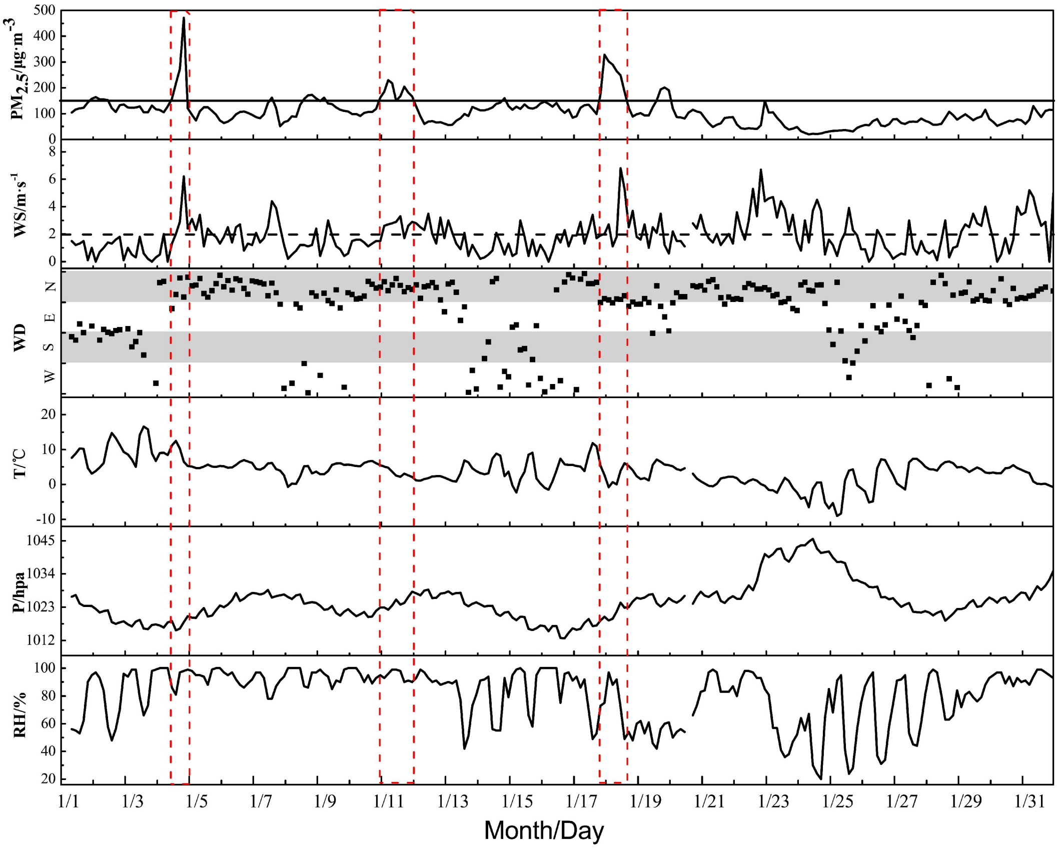

Fig. 3. Hourly variations of meteorological elements and $PM_{2.5}$ concentrations in Wuhan in January 2016 with heavy air pollution periods marked with the columns in red dash lines and $PM_{2.5}$ concentrations exceeding 150 $\mu g \cdot m^{-3}$ (solid line).

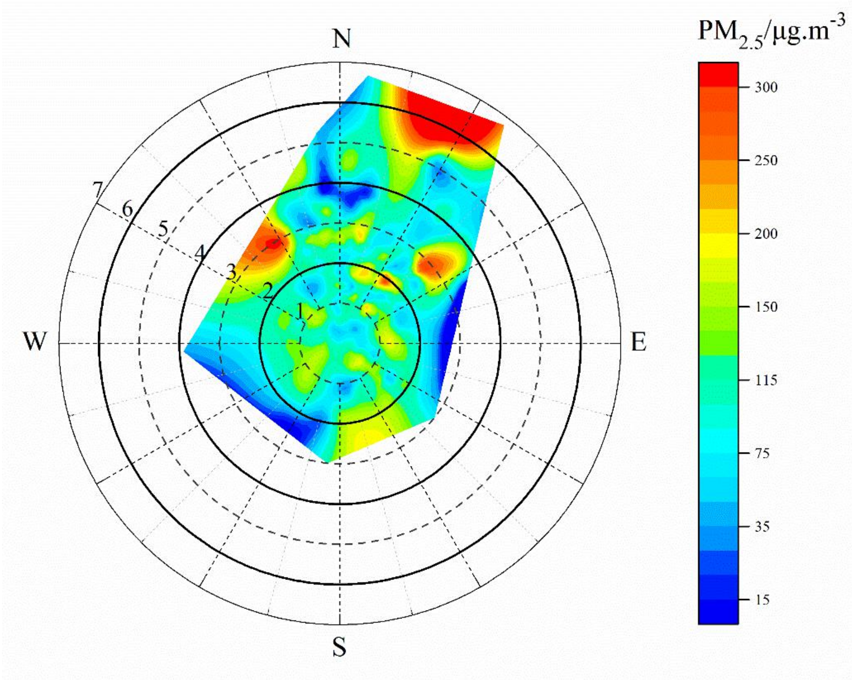

Fig. 4. A polar plot of hourly variations in wind speed (round radius, units is $m \cdot s^{-1}$) and direction (angles) to surface $PM_{2.5}$ concentrations (color contours, units is $\mu g \cdot m^{-3}$) in Wuhan in January, 2016.

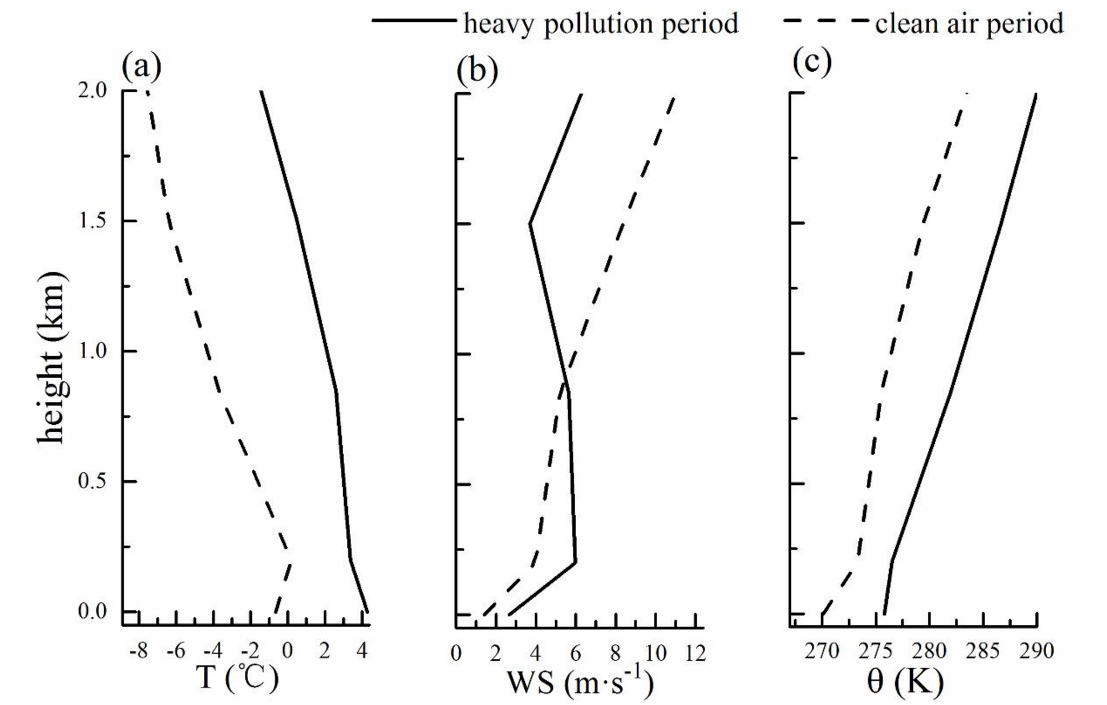

Fig. 5. Vertical profiles of (a) air temperature, (b) wind velocity and (c) potential temperature

averaged in heavy $PM_{2.5}$ pollution and clean air periods over Wuhan during January 2016.

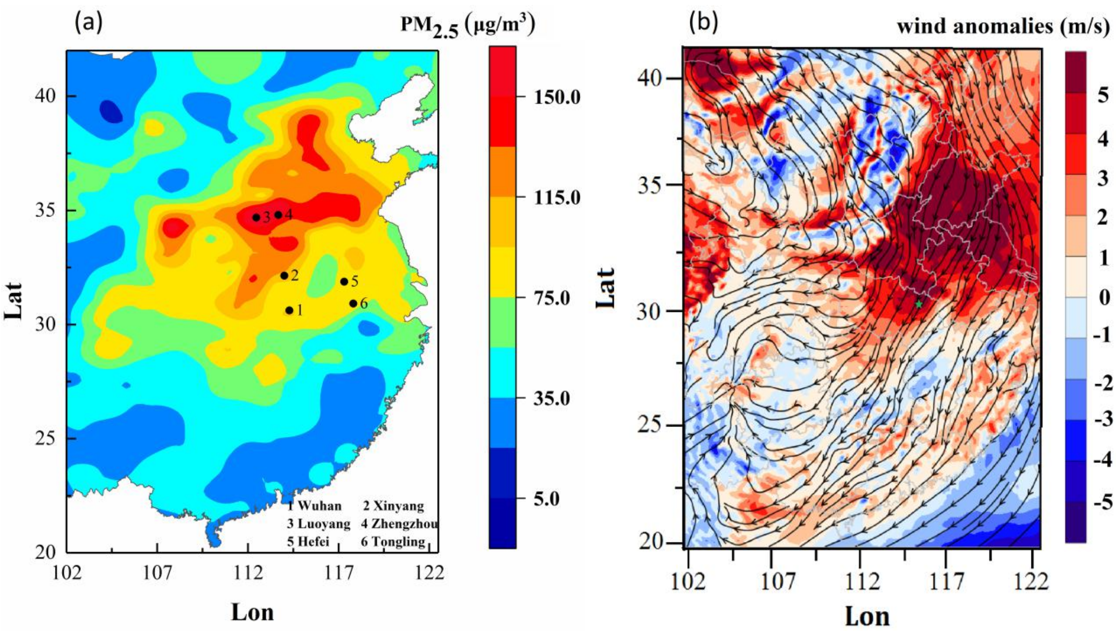

Fig. 6 Distribution of (a) monthly averages of surface $PM_{2.5}$ concentrations observed in January 2016 over central-eastern regions in mainland China with the locations of six sites 1. Wuhan, 2. Xinyang, 3. Luoyang, 4. Zhengzhou, 5. Hefei and 6.Tongling as well as (b) the anomalies (color contours) of 200m wind speeds averaged during three heavy air pollution periods relatively to the monthly wind averages (streamlines) in January 2016 over central-eastern China with the location of Wuhan (a light blue star).

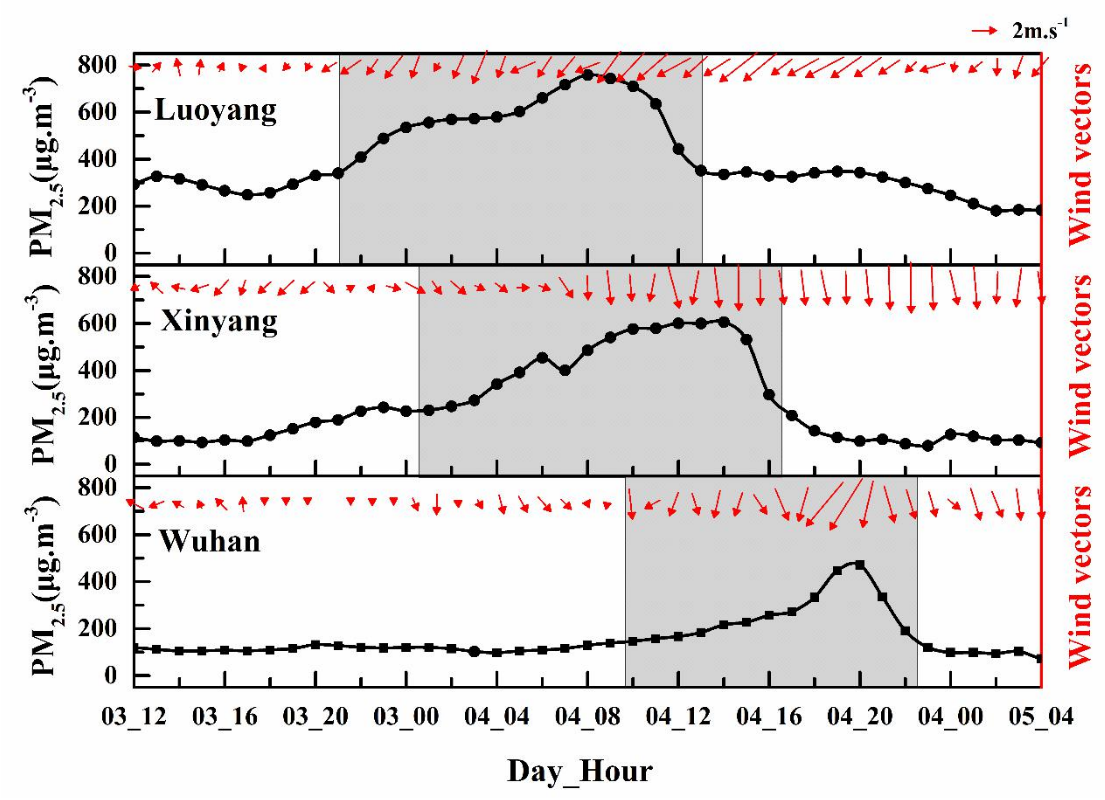
2m.s-1
Luoyang
Xinyang
Wuhan
PM2.5(μg.m-3)
Wind vectors
03_12
03_16
03_20
03_00
04_04
04_08
04_12
04_16
04_20
04_00
05_04
Day_Hour

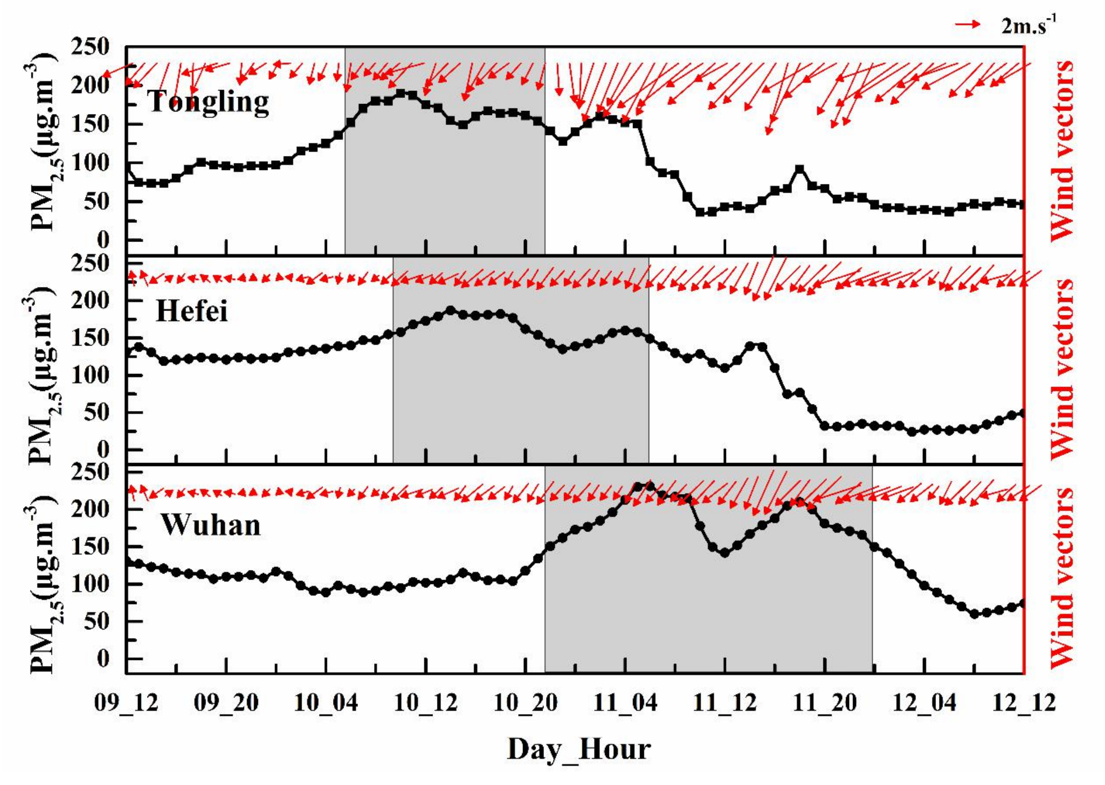
2m.s-1
Tongling
Hefei
Wuhan
PM2.5(μg.m-3)
Wind vectors
09_12
09_20
10_04
10_12
10_20
11_04
11_12
11_20
12_04
12_12
Day_Hour

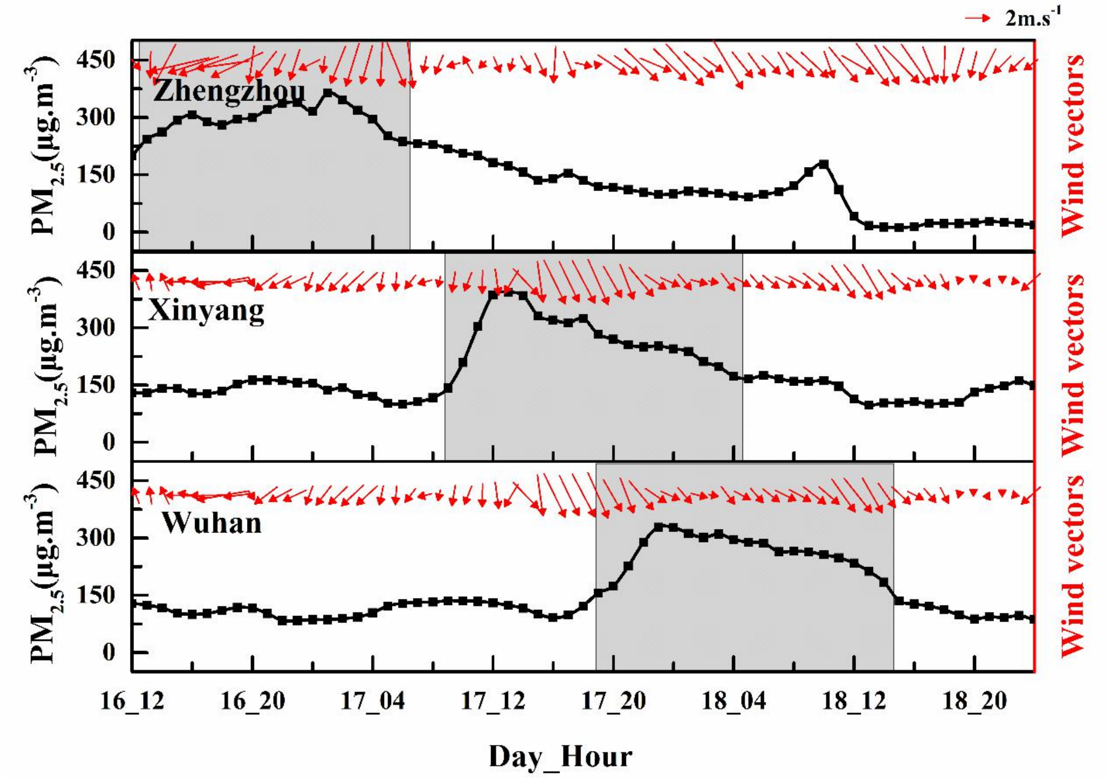

Fig. 7. Temporal changes of $PM_{2.5}$ concentrations (dot lines) and near-surface winds (vectors) observed at five upstream sites (Fig. 6) and Wuhan with shifts of $PM_{2.5}$ peaks (marked with shaded areas) to the YRMB's heavy $PM_{2.5}$ pollution periods P1 P2 and P3 (respectively in upper, middle and lower panels) in January 2016.

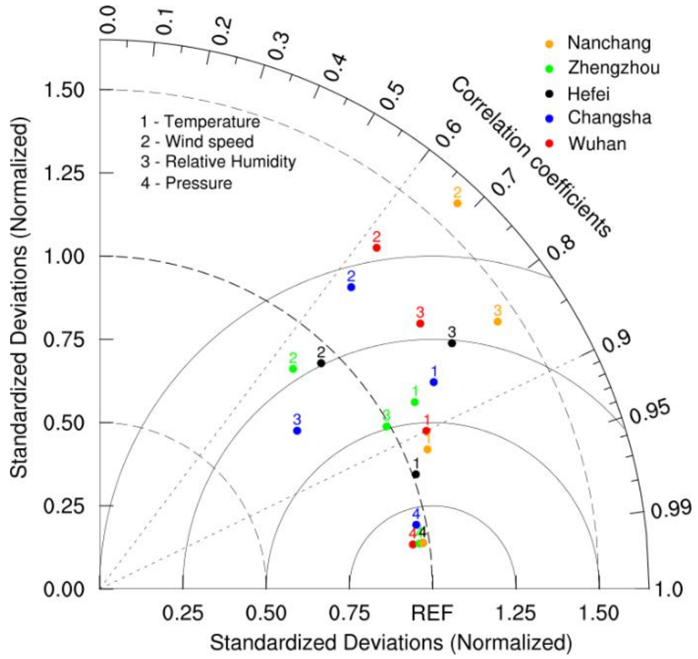

Fig. 8. Taylor plots with the normalized standard deviations and correlation coefficients between simulated and observed meteorological fields. The radian of the sector represents the correlation coefficient, the solid line indicates the ratio of standard deviation between simulations and observations, the distance from the marker to “REF” reflect the normalized root-mean-square error (NRMSE).

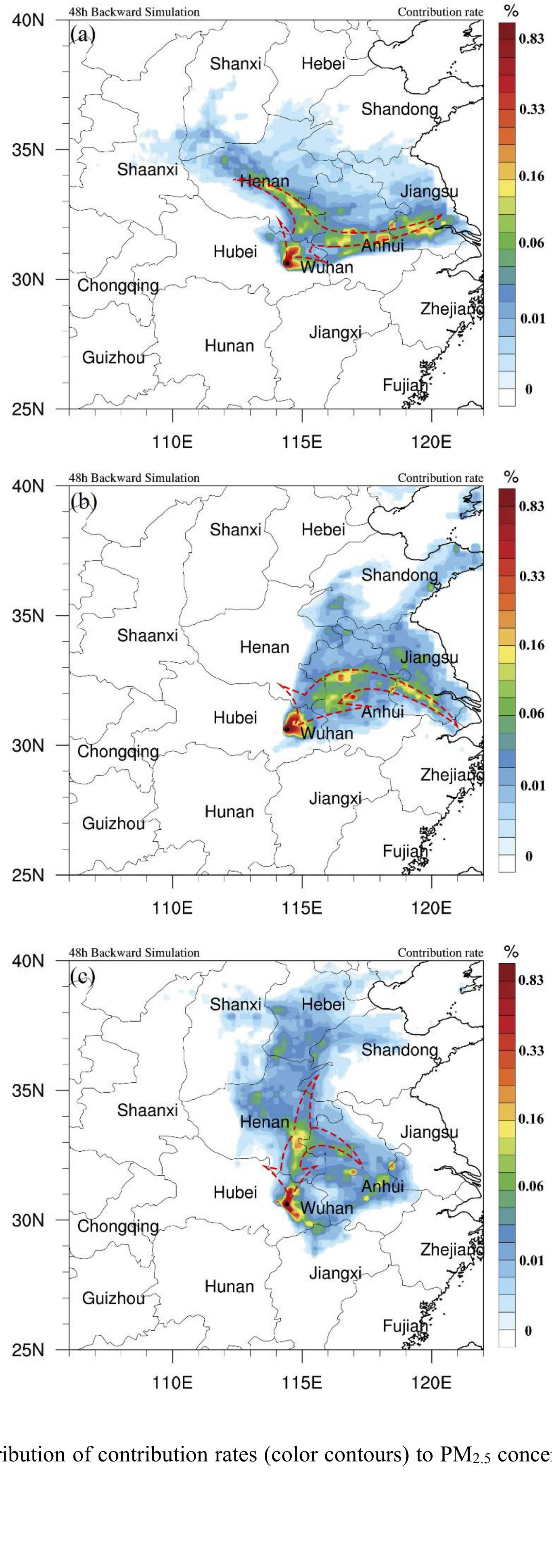

727

728 **Fig. 9.** Spatial distribution of contribution rates (color contours) to $PM_{2.5}$ concentrations in Wuhan

with the major pathways of regional ~~$PM_{2.5}$~~ transport over central-eastern China (dash arrows) for (a) heavy pollution periods P1, (b) P2 and (c) P3 in January, 2016 simulated by the model FLEXPART-WRF.